Journal of Hazardous Materials 425 (2022) 127997

Contents lists available at ScienceDirect

Journal of Hazardous Materials

journal homepage: www.elsevier.com/locate/jhazmat

The influence of drinking water constituents on the level of microplastic release from plastic kettles

Yunhong Shi [a,b,1], Dunzhu Li [a,b,1], Liwen Xiao [b,c,*], Emmet D. Sheerin [a,d], Daragh Mullarkey [a,e], Luming Yang [a,b], Xue Bai [a,d], Igor V. Shvets [a,e], John J. Boland [a,d,**], Jing Jing Wang [a,***]

[a] AMBER Research Centre and Centre for Research on Adaptive Nanostructures and Nanodevices (CRANN), Trinity College Dublin, Dublin 2, Ireland
[b] Department of Civil, Structural and Environmental Engineering, Trinity College Dublin, Dublin 2, Ireland
[c] TrinityHaus, Trinity College Dublin, Dublin 2, Ireland
[d] School of Chemistry, Trinity College Dublin, Dublin 2, Ireland
[e] School of Physics, Trinity College Dublin, Dublin 2, Ireland

ARTICLE INFO

Editor: Dr. T Meiping

Keywords:
Microplastics release
Kettles
Water hardness
Ions
Films

ABSTRACT

Microplastic (MP) release from household plastic products has become a global concern due to the high recorded levels of microplastic and the direct risk of human exposure. However, the most widely used MP measurement protocol, which involves the use of deionized (DI) water, fails to account for the ions and particles present in real drinking water. In this paper, the influence of typical ions (Ca^{2+}/HCO_3^-, Fe^{3+}, Cu^{2+}) and particles (Fe_2O_3 particles) on MP release was systematically investigated by conducting a 100-day study using plastic kettles. Surprisingly, after 40 days, all ions resulted in a greater than 89.0% reduction in MP release while Fe_2O_3 particles showed no significant effect compared to the DI water control. The MP reduction efficiency ranking is $Fe^{3+} \approx Cu^{2+} > Ca^{2+}/HCO_3^- > > Fe_2O_3$ particles ≈ DI water. Physical and chemical characterization using SEM-EDX, AFM, XPS and Raman spectroscopy confirmed Ca^{2+}/HCO_3^-, Cu^{2+} and Fe^{3+} ions are transformed into passivating films of $CaCO_3$, CuO, and Fe_2O_3, respectively, which are barriers to MP release. In contrast, there was no film formed when the plastic was exposed to Fe_2O_3 particles. Studies also confirmed that films with different chemical compositions form naturally in kettles during real life due to the different ions present in local regional water supplies. All films identified in this study can substantially reduce the levels of MP release while withstanding the repeated adverse conditions associated with daily use. This study underscores the potential for regional variations in human MP exposure due to the substantial impact water constituents have on the formation of passivating film formation and the subsequent release of MPs.

1. Introduction

Microplastics (MPs) are a global concern due to the potential risk to human health and to the environment. Household plastic products (e.g., plastic lunchbox (He et al., 2021), plastic-laminated disposable cup (Ranjan et al., 2020) and baby feeding bottle (Li et al., 2020)) have recently been confirmed as local and immediate sources of MP exposure, with millions of MPs released per liter of water. Given the high levels of MP release and the pervasive use of plastic products in daily life, it is not surprising that MPs have been found in human tissue (placenta of pregnant women (Ragusa et al., 2021) and colon (Ibrahim et al., 2021) and human stool (Schwabl et al., 2019)). Although the specific risk to human health is not yet known, MP exposure was reported to induce gut microbiota dysbiosis and lipid metabolism disorder in mice (Jin et al., 2019; Lu et al., 2018). Researchers have also found that sub-micron MPs with the sizes of 52–330 nm can penetrate the blood-to-brain barrier and cause behavioural disorders in fish (Mattsson et al., 2017). A recent study using macrophage cells pointed out that the cellular

* Corresponding author at: Department of Civil, Structural and Environmental Engineering, Trinity College Dublin, Dublin 2, Ireland.
** Corresponding author at: AMBER Research Centre and Centre for Research on Adaptive Nanostructures and Nanodevices (CRANN), Trinity College Dublin, Dublin 2, Ireland.
*** Corresponding author.
E-mail addresses: liwen.xiao@tcd.ie (L. Xiao), jboland@tcd.ie (J.J. Boland), jjwang@tcd.ie (J.J. Wang).
[1] For equal contributions

https://doi.org/10.1016/j.jhazmat.2021.127997
Received 12 August 2021; Received in revised form 2 December 2021; Accepted 3 December 2021
Available online 6 December 2021

internalization capacity is likely to be a major source of toxicological risk of MPs (Ramsperger et al., 2020). Pristine MPs can absorb biomolecules after exposure to fresh and salt water, which enhances MP uptake in cells (Galloway et al., 2017; Ramsperger et al., 2020). Since many plastic products are specifically designed as containers of biomolecule-rich materials (e.g., beverages, soups and foods), it is likely that the MPs released from these products will be exposed to biomolecules, further raising concerns about the potential impact on human health.

Deionized (DI) water (Du et al., 2020; Fadare et al., 2020; Li et al., 2020; Ranjan et al., 2020; Sturm et al., 2019) or similar purified types of water (Hernandez et al., 2019) is widely used in established protocols to quantify MPs release from daily-use plastics. However, DI water is rarely used outside of laboratory. During real world use, plastic products come into contact with drinking water, which is a universal solvent containing many species of ions and particles. For example, the mean hardness of water sources in US is 217 mg/L (as $CaCO_3$), while some regions (e.g., Texas and New Mexico) report levels higher than 1000 mg/L (Briggs and Ficke, 1977). In addition to Ca^{2+} and HCO_3^- ions in hard water, many other types of ions, such as Fe^{3+} and Cu^{2+}, are ubiquitous in drinking water, because iron and copper are the top two most widely used materials for plumbing and piping of drinking water (WHO, 2006). In addition to ions, solid particulate matter is also known to widely exist in drinking water. For example, Fe_2O_3 particles are commonly found in tap water due to the corrosion of iron pipelines (Sarin et al., 2004). Size distribution analysis found that most particles are within the 0.9–16 μm range (Pronk et al., 2007). It is well known that hard water usually results in limescale films being generated on the surfaces of exposed items, which may influence MP release. Similar effects may also occur when surfaces of plastic products are routinely exposed to water containing particulate matter. However, to date, there has been no systematic investigation of the influence ions and particles commonly found in drinking water on the release of MPs from plastic products.

Plastic kettles are one of the most widely used household appliances. Sales data shows that polypropylene (PP) kettles accounts for 83.0% of the total market (Fig. 1, data mined from Amazon ecommerce sites from nine countries). A study involving plastic kettles reported that up to 30 million particles are released per liter of water during the boiling process (Sturm et al., 2019), demonstrating that plastic kettles are a potentially significant source of MP exposure. However, the previous study focussed on MP release from brand-new kettles using DI water (Sturm et al., 2019). Since a typical kettle is repeatedly exposed to real tap water during hundreds of boil cycles, it is important to investigate the long-term effects of water that contains typical concentrations of ions and particles on the level of MP release.

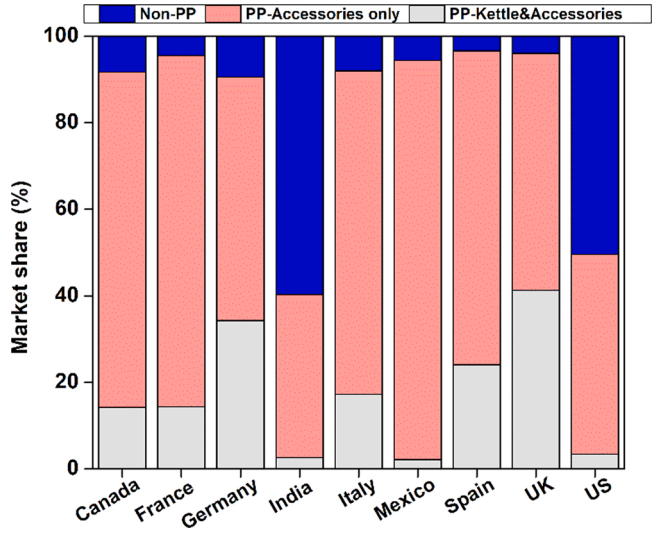

Fig. 1. The market share of PP kettles in 9 countries (PP kettle & accessories: both the kettles body and accessories are made of PP; PP-Accessories only: includes only kettle accessories that are made of PP, such as PP filters, PP water scales and PP lids; Non-PP: neither the kettle body or the accessories are made of PP, such as glass kettles and stainless kettles).

To investigate the influence of water constituents on MP release, four synthetic drinking waters containing different typical ions (Ca^{2+}/HCO_3^-; Fe^{3+} and Cu^{2+}) and particles (Fe_2O_3 particles) were prepared and used to boil plastic kettles. Raman spectroscopy testing was conducted to monitor MP release from kettles boiled using these different types of water. In addition, physical and chemical characterization using SEM-EDX, AFM, XPS and Raman spectroscopy was also employed to study the change in the morphology of the exposed kettle surface. Surprisingly, all ions achieved at least 89% reduction in MP release while particles showed no significant reduction when compared to kettles exposed to DI water. Physical and chemical characterization confirmed the ions in the different water types resulted in the formation of passivation films on the exposed kettle surface, each of which led to a substantial reduction in MP release level over that found for DI water. In contrast, no film was formed when the plastic was exposed to the synthetic water with particles (Fe_2O_3). This study underscores the substantial influence water constituents have on the regional levels of MP release and the potential for human exposure.

2. Methods and materials

2.1. Precautions to prevent sample contamination and control samples

To avoid any potential contamination, this study followed an established and independently validated protocol (Li et al., 2020, 2021). Clean cotton-based laboratory coats and pre-washed particle-free nitrile gloves were worn at all times. Clean boro 3.3 glassware was used for sample preparation. The prepared samples were immediately placed in the glass petri dish (Brand™, FisherScientific) before Raman testing and analysis. DI water with resistivity of 18.2 MΩ-cm was used. Control samples were also run every ten samples to ensure the contamination-free protocol was being adhered to.

For the control sample, a glass beaker with a glass cover was filled with 50 mL DI water and boiled for 2.5 mins using a hotplate. After cooldown, any particles present in the water were filtered and checked for MP contamination using Raman spectroscopy.

2.2. Preparation of synthetic drinking water

Four types of synthetic drinking water (SDW) were investigated - hard water containing Ca^{2+} and HCO_3^-; Fe^{3+} water containing $FeCl_3$; Cu^{2+} water containing $CuSO_4$ and particle water containing Fe_2O_3 particles. Each was prepared by adding a measured quantity of these compounds to DI water. While the chemical composition of drinking water varies locally, the WHO has prescribed a drinking water safety standard that sets the recommended allowable concentration ranges for various ions, particles and organics (WHO, 2011). For example, the suggested concentration of copper is not to be higher than 2 mg/L. Hence, and Cu^{2+} water was prepared by adding 5.0 mg/L-$CuSO_4$ to (i.e., 2 mg/L-Cu element) in DI water. Accordingly, the concentration of elemental iron in Fe^{3+} water and particle water were both adjusted to 2 mg/L to allow results to be compared. To mimic particles found in drinking water, Fe_2O_3 particles with an average size of 5.4 μm (97% of particles are in size range 1.2–16 μm, Fig. S1) were used. These particles closely match the real particle size distribution found in drinking water (0.9–16 μm (Pronk et al., 2007)). Following hard water classification and reported typical compositions (Briggs and Ficke, 1977), synthetic hard water containing ions of Ca^{2+}/HCO_3^- was prepared by adding $CaCl_2$ and $KHCO_3$, so that the hardness was adjusted to 180 mg/L-$CaCO_3$. In addition, quantities of KCl, $Mg(NO_3)_2.6\,H_2O$ and humic acid sodium salt (to simulate organic content) was also added to

the synthetic drinking water to mimic local (Dublin, Ireland) drinking water composition. In compliance with the WHO standard (WHO, 2011), the pH of SDW was finally adjusted to 7.5–8.5 range using NaOH solution. The specific composition of each type of SDW used in this study is listed in Table 1.

2.3. 100-day test using different water types

To investigate the influence of ions and particles on MP release, a popular plastic kettle product (120,000 of units sold annually in Amazon UK alone) was chosen as a representative plastic product to conduct a 100-day test. Five identical brand-new kettles were tested for each water type as well as DI water (as the benchmark control). All kettles were cleaned thoroughly using DI water before testing. Then the kettles were filled with 0.8 L of as-prepared SDW water or DI water and boiled once per day in accordance with a survey of average kettle users and rinsed with DI water before the next boil (Murray et al., 2016).

To quantify the MP release levels, an extra boil was performed on Day 0, 1, 3, 5, 10, 15, 20, 30, 40, 50, 60, 70, 80, 90 and 100 in which DI water was used to collect the released MPs (Fig. 2). It is well established that exposure to DI water does not lead to the dissolution or growth of any pre-existing passivation film present on the plastic surface (Li et al., 2020) and its use facilitates MP analysis by eliminating potential sources of contamination present in real tap water. Hence, DI water was used to test MP release from kettles that had been boiled using different water types during the 100-day test. In the case of these extra boils, the boiled DI water sample was collected, filtered and analyzed using the established protocol (Li et al., 2020). In brief, the water samples containing MPs were allowed to cool down to room temperature. Then the water samples were gently shaken and filtered through the gold-coated polycarbonate membrane filter (APC, Germany Ltd). The diameter of membrane filter was 25 mm with a pore size of 0.8 μm.

2.4. Test of new and used kettles under real world conditions

To demonstrate the natural occurrence of passivation films from different water types, used kettles were randomly collected from soft water (Dublin, hardness around 50 mg/L as $CaCO_3$) and hard water (Kildare, around 170 mg/L as $CaCO_3$) supply zones (information listed in Table 2). MP release levels from these used kettles was tested following the protocol in Fig. 2b. The particles on the surfaces of the used kettle interiors were also investigated using Raman spectroscopy. To assess the level of MP suppression follow real world use, brand new kettles of the same kind were purchased and separately tested (for test method see Fig. 2b).

2.5. Identification and quantification of MPs using Raman spectroscopy

The chemical identity of particles released from the plastic kettles was determined by Raman spectroscopy (Renishaw InVia Raman spectrometer) with the detection limit down to 1 μm following established test protocols (Käppler et al., 2016; Li et al., 2020). The system consists of a 532-nm laser (Coherent), a cooled charge-coupled device and a microscope with a 100 × objective. The WiRE 3.4 (Renishaw) software was used for detection. Before each test, a silicon wafer was used to calibrate the system. For MP identification, a low-excitation laser power was applied to avoid potential damage to the particles. Spectra were obtained over the range 200–3200 cm^{-1}. Intensive Raman peaks in the ranges of 2780–2980, 1400–1640 and 709–850 cm^{-1} were used to determine the chemical composition of MPs in this study. Fig. S2 shows the Raman spectra from the bulk kettle and the level of released PP-MPs, respectively. The quantity and size distribution of the PP-MPs were analysed by ImageJ software, following established protocols (Käppler et al., 2016; Li et al., 2020).

Table 1
The chemical composition of different types of water used in the study.

Water type	SDW-Cu^{2+} mg/L	SDW- Ca^{2+}/HCO_3^- mg/L	SDW-Fe^{3+} mg/L	SDW-Fe_2O_3 mg/L	DI mg/L
$C_9H_8Na_2O_4$ (sodium humic acid)	0.1	0.1	0.1	0.1	0
$Mg(NO_3)_2.6\ H_2O$	13.2	13.2	13.2	13.2	0
KCl	1.9	1.9	1.9	1.9	0
$CuSO_4$	5.0	0	0	0	0
$CaCl_2$	7.0	166.5	7.0	7.0	0
$KHCO_3$	0	300.0	0	0	0
$FeCl_3$	0	0	5.8	0	0
Fe_2O_3	0	0	0	2.9	0

2.6. Characterization of the inner surface of kettles

Multiple techniques were to characterize physiochemical change of the kettle's inner surface. SEM-EDX (Zeiss Ultra Plus) was performed with an acceleration voltage of 15 kV. High-resolution XPS was performed using an Omicron Multiprobe XPS with a monochromated Al K-alpha source. A low energy electron flood gun was used during all XPS measurements to compensate for surface charging. Raman spectroscopic testing (Renishaw InVia Raman spectrometer) was also conducted with 532 nm excitation laser and 50% laser intensity to determine the chemical identity of the particles/films on the inner kettle surface. 3D images of kettle surfaces were acquired using atomic force microscopy (AFM, NT-MDT) using a tapping mode probe (Nanosensors, PPP-NCST). The system was calibrated using step height standard (SHS) while the results were analyzed using Gwyddion 2.54 software.

3. Results

3.1. Ions influence MPs release

Given the well-known classification of hard/soft water as well as the ubiquitous presence of iron and copper ions in drinking water, four water types (Ca^{2+}/HCO_3^- SDW; Fe^{3+} SDW, Cu^{2+} SDW and DI water) were used to investigate the influence of ionic species on MP release. The general trend in MP release from Fe^{3+} water, Cu^{2+} water and Ca^{2+}/HCO_3^- water is significantly different from that observed for kettles boiled using DI water (Fig. 3). During the first 15-days of use, MP numbers associated with each water type decreases from an initial level of 25.0–35.0 million/L to around 5.0–10.0 million/L (Fig. 3a). After that, MP numbers for DI boiled kettle increased to 15.0 million/L after 40 times boils while SDW with different ions continuously decreased to between 2.5 and 5.0 million/L. To account for differences in the initial MP release level for different water types, the data was normalised by setting the initial release number for each water type to 100% (Fig. 3b). After repeated use (after 20 boils), the DI-water boiled kettles always released over 10.0 million/L, which equivalent to 40.0–60.0% of the initial release number. In comparison, SDW boiled kettles released significantly lower MP levels regardless of the ion type. After 40 boils, all kettles released less than 11.0% of the initial values. The SDW containing Fe^{3+} ions gave the largest suppression, with a reduction of 96.9% after 100 boils. Ca^{2+}/HCO_3^- water achieved a slightly reduced level of suppression, with an 89.7% reduction after 100 boils, while Cu^{2+} resulted in a reduction of 94.5%.

Evidently, the 3 groups of common ions found in drinking water all showed an ability to substantially reduce to the level of MP release, with Fe^{3+} water showing the highest reduction.

3.2. Element speciation (ion and particle) influence MPs release

To have an in-depth understanding of this MP suppression phenomenon, two types of iron-containing species (ion-Fe^{3+} and particle-Fe_2O_3) were chosen to investigate the influence of chemical speciation.

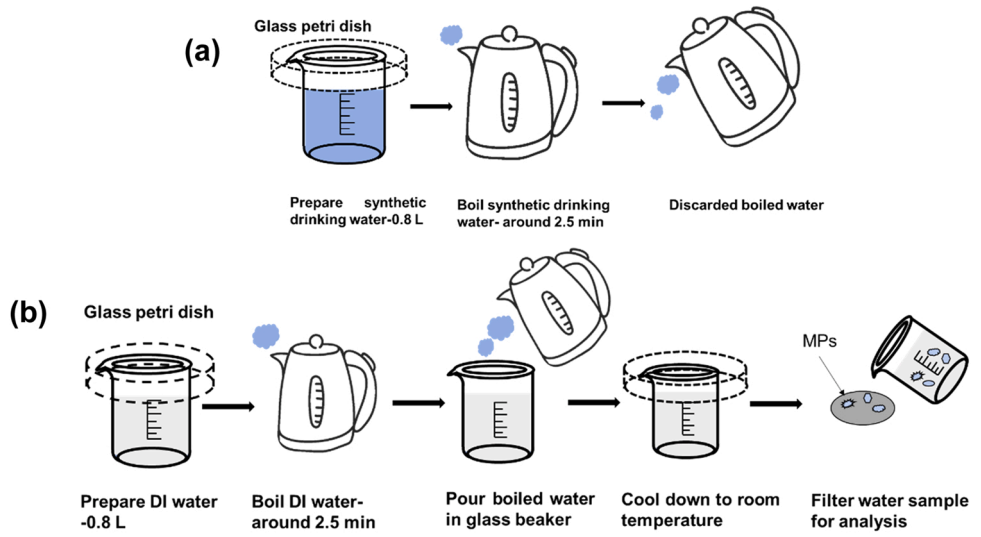

Fig. 2. MPs sample preparation protocol. (a) Water boils process using SDW or DI in 100 days. (b) Schematic detailing the methodology used to determine MP release level during the extra boil with DI water. To avoid any potential MP residual due to last boil, the kettle was gently rinsed using DI water before each extra test boil.

Table 2
The information of three used kettles operated under real-world conditions.

Product	Service time[a]	Approx. use times per day[a]	Approx. total use times[a]	Water hardness[b]
K1	1 month	1	30	170.0 mg/L
K2	24 months	0.5	400	50.0 mg/L
K3	3 months	2	200	50.0 mg/L

[a] : the data obtained by surveying the kettles' users, which is the approximate use times and total use rimes; b: hardness as CaCO3, data obtained from Irish Water-https://www.water.ie/help/water-quality/hard-water/

Surprisingly, MP release levels for Fe_2O_3-particle (Fe-P) containing water showed very similar trends to that of DI water (Fig. 4a and Fig. S3a), indicating that particles of Fe_2O_3 have a weak effect on MP release. The normalized release data shows that only after Day 70 the MP release level from Fe-P water kettles started to drop below that of DI boiled kettle (Fig. 4a). On Days 70–100, Fe-P reduced the level of MP release by about 60.2%, while the value for DI water was around 52.0%. These results are in sharp contrast to the reduction of 96.9% found for Fe^{3+} water (Fig. 4a). Evidently, the speciation of the element substantially influences the level of MP suppression.

The size distribution of the released MPs was also investigated. For kettles exposed to DI water, the initially released particles that are in the < 5 μm, 5–10 μm and > 10 μm ranges were 79.3%, 10.9% and 9.8% of the total particles, respectively (Fig. 4b). After 100-day of boiling, the particle distribution did not change significantly. In comparison, the size of MPs released from Fe^{3+} water boiled kettles showed substantial differences (Fig. 4c). After 100-day of boiling, the particles within 5–10 μm and > 10 μm ranges decreased from 23.2% and 23.2–15.0% and 1.3%, respectively. Similar changes were also observed for kettles boiled using Fe-P water (Fig. S3b). These results indicate that ions and particles likely change the kettle surface to ways that act to limit the release of large MPs.

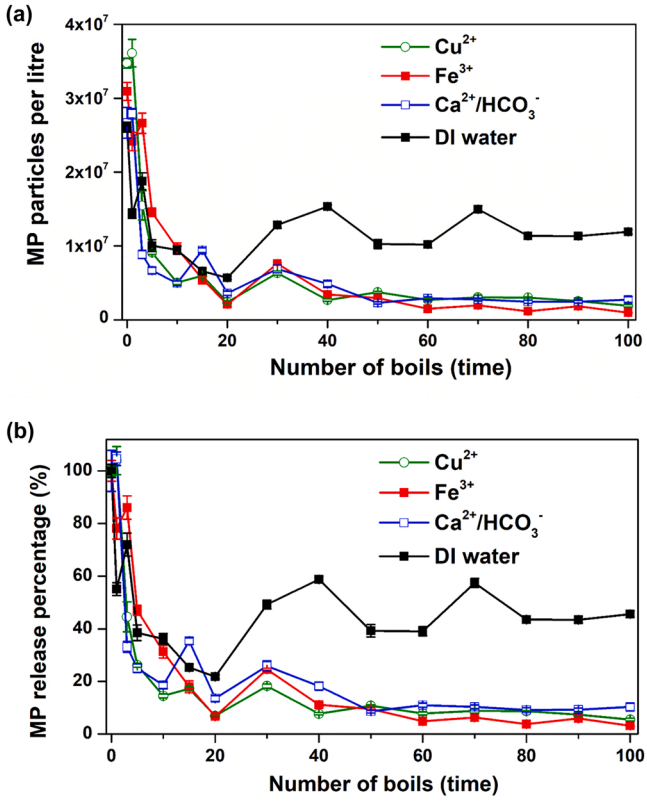

Fig. 3. (a) Long-term test of the correlation between boils number and MPs release number using Cu^{2+} water, Fe^{3+} water, Ca^{2+}/HCO_3^- water and DI water, respectively. (b) Long-term test of the correlation between boils number and MPs release level (%) using Cu^{2+} water, Fe^{3+} water, Ca^{2+}/HCO_3^- water and DI water, respectively. Normalizing all data by dividing by the first day release level.

3.3. Morphology analysis of kettle surface

To understand the origin of this MP suppression phenomenon, the inner surfaces of kettles before and after 100-day test were characterized using AFM and SEM. In the case of DI-water boiled kettles the surface after the test is similar to that of a brand-new kettle (Fig. 5a and b). Though some particles were observed, these surfaces were relatively clean and smooth. However, for SDW exposed kettles, the inner surfaces showed substantial changes (Fig. 5c-f). The Ca^{2+}/HCO_3^- water exposed surface was rich with tiny rods, with lengths of around 10^1-10^2 μm. High resolution imaging showed that the Cu and Fe ion-exposed surfaces were covered with a continuous film. The Fe-P water boiled kettles had the

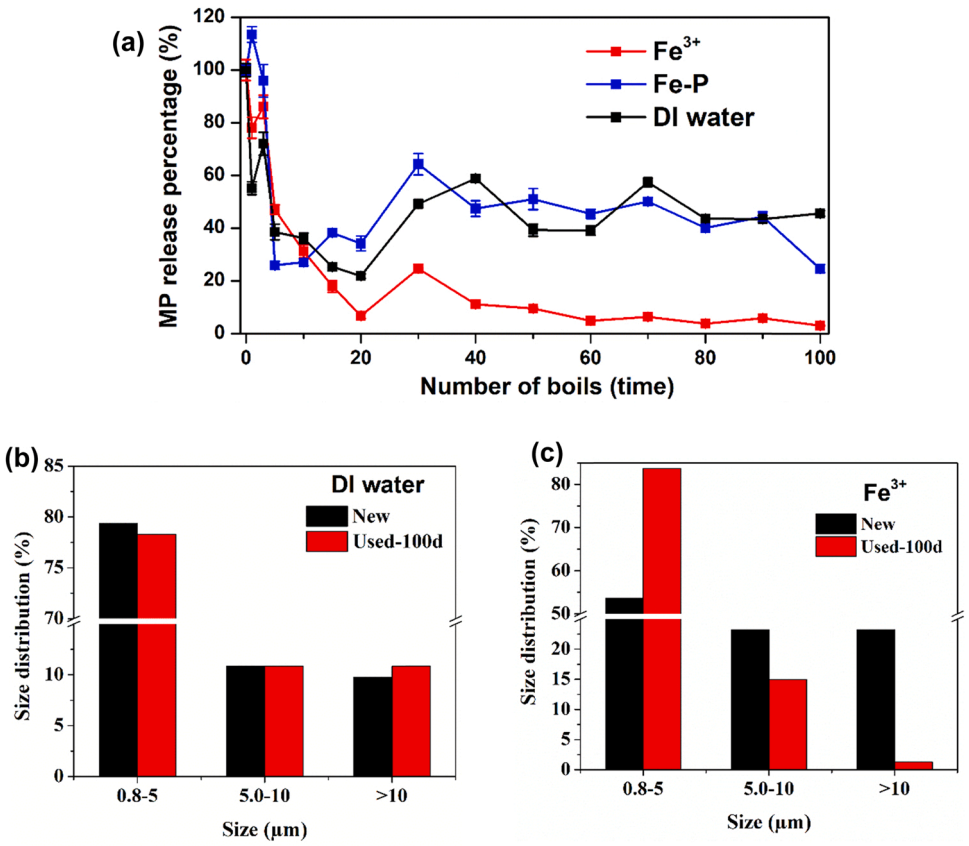

Fig. 4. (a) Long-term test of the correlation between boils number and MPs release level (%) using Fe^{3+} water, Fe-P water and DI water, respectively. Normalizing all data by dividing by the first day release level. The size distribution of release MP from kettles boiled by (b) DI water and (c) Fe^{3+} water, respectively.

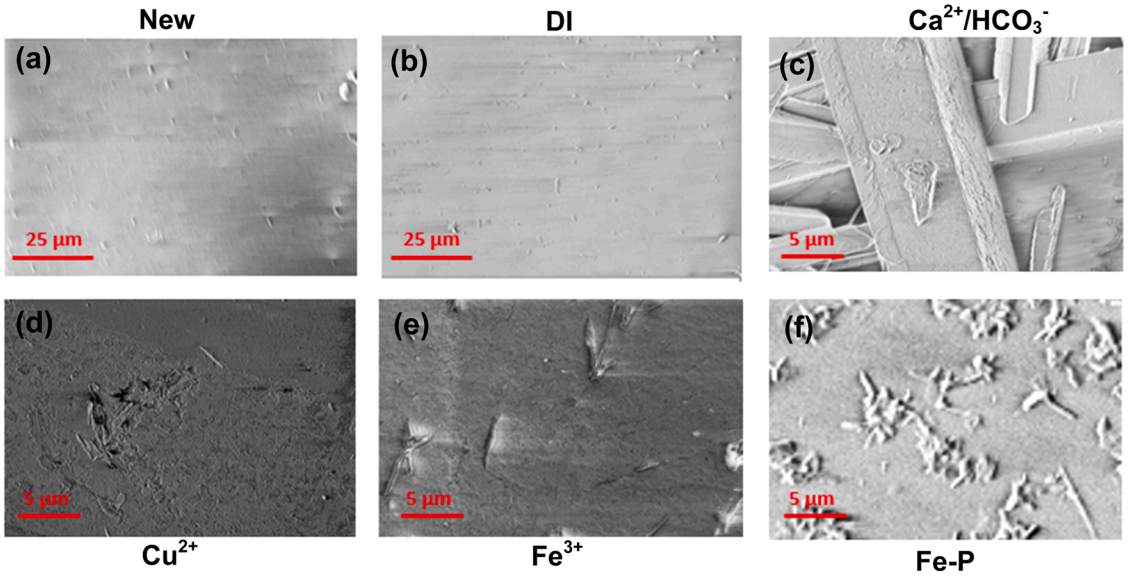

Fig. 5. SEM images (a-f) of the inner surface of new kettle and 100-day boiled kettle using DI water, Ca^{2+}/HCO_3^-water, Cu^{2+} water, Fe^{3+} water, and Fe-P water, respectively.

coarsest surface, that was covered by numerous irregular particles. However, these particles were discrete and no evidence of a continuous film was found.

AFM testing was conducted to study the detailed surface morphology (Fig. 6 and Fig. S4). Most features observed on the surface of new kettles and kettles exposed to DI water were less than 500 nm in height (Fig. S4). The height of the small rods observed following Ca^{2+}/HCO_3^- water exposure were around 2 μm. For surfaces exposed to Fe^{3+} water and Cu^{2+} water, continuous and coarse films were formed. Surfaces exposed to boiling Fe-P water, were partially covered by aggregated

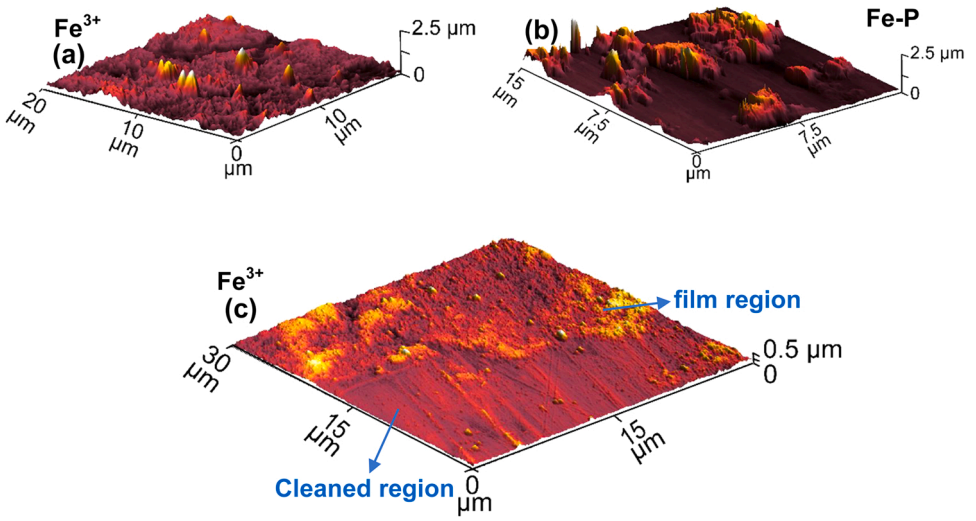

Fig. 6. AFM images (a-b) of the inner surface of 100-day boiled kettle using Fe^{3+} water and Fe-P water, respectively. (c) AFM image of partially cleaned surface of 100-day boiled kettle using Fe^{3+} water. To confirm the formation of Fe_2O_3 film on Fe^{3+} water exposed kettle, piece of exposed kettle was taken and gently rinsed using DI water. Then part of the surface was carefully removed using lens clean paper. After that, the surface was investigated using AFM.

particles with lateral sizes of around 2–5 μm with a height of around 1 μm. The absence of continuous film may be the reason for the poor level of MP suppression following Fe-P exposure.

3.4. Chemical characterization of kettle surface

To reveal the chemical nature of the materials adhered onto the kettle surfaces, EDX elemental analysis was conducted. Strong EDX elemental peaks corresponding to calcium-Ca, copper-Cu, iron-Fe and iron-Fe were found in the spectra of Ca^{2+}/HCO_3^- water, Cu^{2+}, Fe^{3+} and Fe-P exposed surfaces, respectively (Fig. 7). In comparison, there were no peaks associated with Ca, Cu and Fe detected on the surfaces of new kettles or those exposed to DI water (Fig. S5). The presence of oxygen and carbon were also confirmed for all surfaces. High-resolution XPS identified the nature of the calcium, copper and iron (Fig. 8). XPS peaks at binding energies of around 352 and 348 eV are consistent with the $Ca2p_{1/2}$ and $Ca2p_{3/2}$ peaks associated with calcium (II), respectively (Fig. 8b). XPS also confirmed that copper (II) was the main speciation given that peaks at binding energies of around 953, 932 and 940–944 eV agree with the standard spectra of $Cu2p_{1/2}$, $Cu2p_{3/2}$ and shake-up satellite peaks associated with copper (II), respectively (Biesinger et al., 2010; Shackery et al., 2016; Van der Laan et al., 1981) (Fig. 8c). For Fe^{3+} exposed surfaces (Fig. 8d), the well-defined peaks of $Fe2p_{1/2}$ and $Fe2p_{3/2}$ associated with iron (III) were found at binding energies of around 724 and 711 eV. Notably, there were no peaks present at 708 and 707 eV, which are associated with iron (II) (Biesinger et al., 2011). The satellite peaks at 717–722 eV were also consistent with iron (III). Collectively, these data confirmed that the majority element iron on Fe^{3+} exposed surface is in the form of iron (III). Although the iron peaks were also observed on Fe-P exposed surfaces, the whole spectrum was much weaker than that of Fe^{3+} exposed surfaces and the signal level was insufficient to determine the precise chemical composition.

Raman spectroscopic analysis of the particles on hardwater exposed surface closely matched the spectrum of calcium (II) carbonate ($CaCO_3$) (Fig. 9a). The significant peaks at around 1086 and 155 cm^{-1}, correspond to the well-known A^1_g, and E_g vibrations of $CaCO_3$. In the case of on Cu^{2+} exposed surfaces strong Raman peaks were observed at around 288, 335 and 625 cm^{-1}, corresponding to the well-known A_g, $B_g^1$and B_g^2 vibrations of CuO (Wang et al., 2017; Xu et al., 1999; Yu et al., 2004) (Fig. 9b). Note the ~10 cm^{-1} difference in the Raman shift for A_g, $B_g^1$and B_g^2 vibrations is common for CuO particles, and is typically attributed to size differences (Murthy et al., 2011). For Fe^{3+} and Fe-P exposed surfaces, both particles exhibited Raman spectra consistent with that for iron (III) oxide (Fe_2O_3, Fig. 9c). Since Raman analysis is very sensitive to the presence of mixed contaminants, the unambiguous data in Fig. 9 confirms that the materials deposited on the inside of kettles following exposure to hard water, and Cu^{2+}, Fe^{3+} and Fe-P water corresponds to $CaCO_3$, CuO, Fe_2O_3 and Fe_2O_3, respectively.

Even though Fe_2O_3 particles are observed on both Fe-P and Fe^{3+}

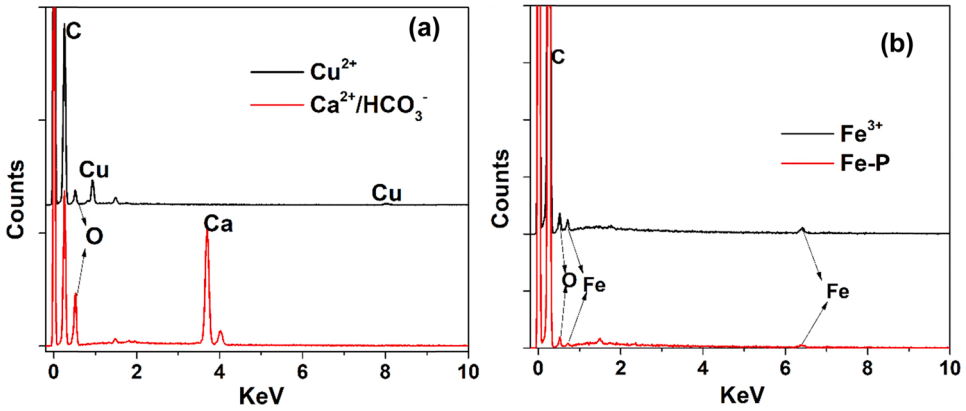

Fig. 7. EDX spectra of the inner surface of 100-day boiled kettle using (a) $Ca^{2+}/HCO_3^-$and Cu^{2+} water; (b) Fe^{3+} water and Fe-P water, respectively.

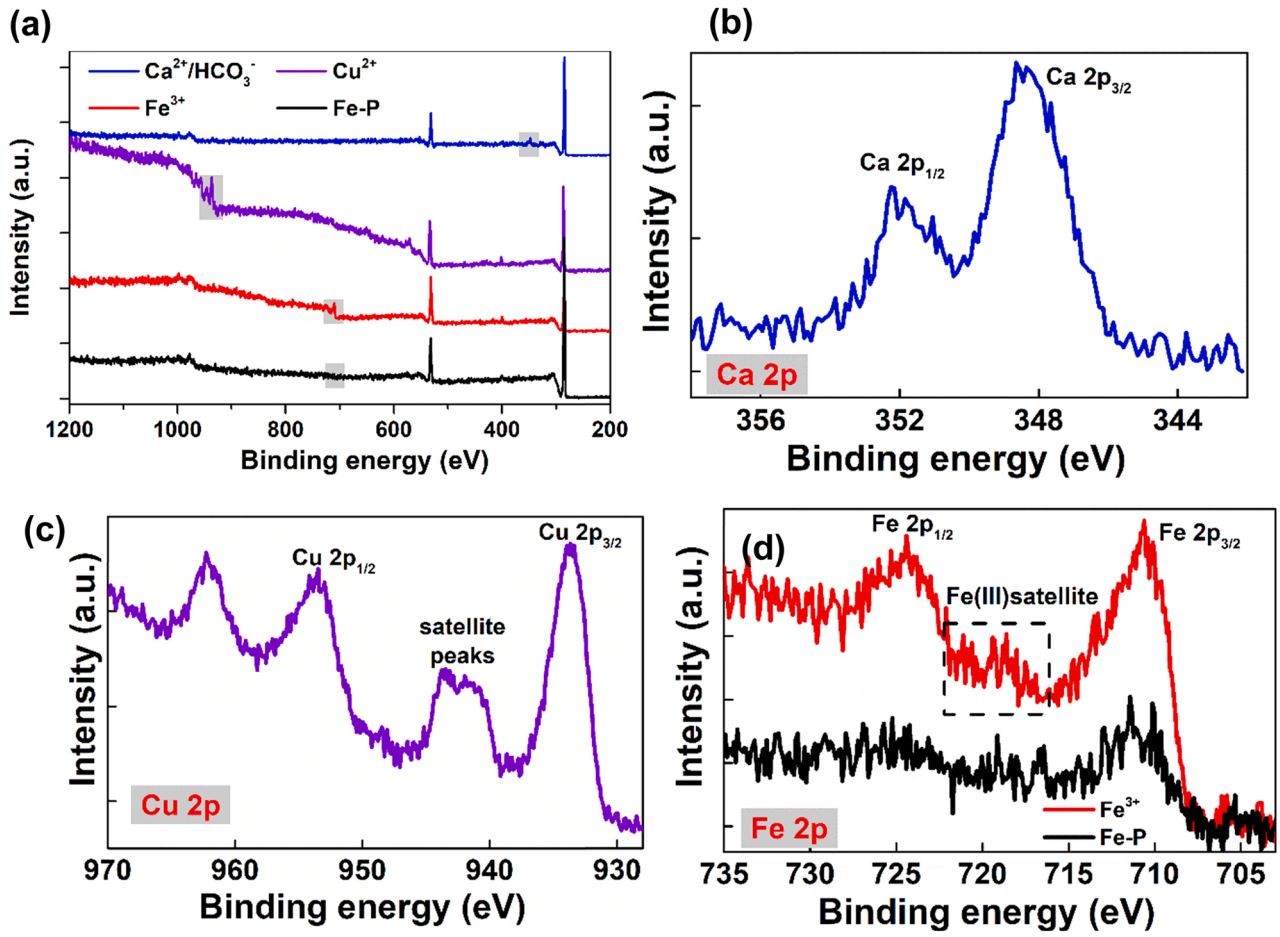

Fig. 8. (a) XPS full spectra of the inner surface of 100-day boiled kettle using HARD, Cu^{2+} water, Fe^{3+} water, and Fe-P water, respectively. (b) zoomed spectra of XPS-Ca 2p of Ca^{2+}/HCO_3^- water boiled surface; (c) zoomed spectra of XPS-Cu 2p of Cu^{2+} water boiled surface; (d) zoomed spectra of XPS-Fe 2p of Fe^{3+} water, and Fe-P water boiled surface, respectively.

exposed surfaces, XPS analysis showed that Fe (III) intensity obtained from Fe^{3+} exposed surface was over 100% stronger than that on the Fe-P exposed surface under the same test conditions (Fig. 8d). EDX analysis also confirms the much stronger intensity of Fe elemental signal obtained from Fe^{3+} exposed surface (Fig. 7b). XPS analysis is very surface sensitive, with penetration depths of only around 10 nm while the lateral size is around 3 mm. EDX analysis can penetrate several μm while the lateral test size here is around 20 μm. SEM and AFM topography analysis showed that the aggregated Fe_2O_3 particles on Fe-P surface were much higher and larger than the particles on Fe^{3+} exposed surface (Figs. 5e-f and 6a-b). Hence, there must be a Fe_2O_3-base film that covers the Fe^{3+} exposed surface. To confirm this, Fe^{3+} exposed kettle surface was partially cleaned and investigated using AFM (Fig. 6c and S5). The resulting cross-section image confirmed that a uniform film with a thickness around 200–300 nm covered the kettle surface. Despite the fact that the initial concentrations of Fe-P and Fe^{3+} were the same, the successful film formation during Fe^{3+} exposure results in the formation of a protective Fe_2O_3 film on the plastic surface that results in a 96.9% reduction in MP release.

Evidently, common ions, such as Fe^{3+}, Cu^{2+}, Ca^{2+} and HCO_3^- in drinking water are transformed into insoluble/slightly soluble compounds, which subsequently form a film that covers the surface of plastic. The potential transformation processes are listed in Eqs. 1–6. During these chemical reactions, generated particles, such as Fe_2O_3 normally grows from the nanometre scale and can easily attach at imperfections on the kettle surface, resulting ultimately in the formation of a continuous and relatively uniform film. However, when the plastic surface is exposed to SDW containing Fe-P particles with an average size of around 5 μm (size distribution see Fig. S1), these particles can only aggregate at random locations on the surface. Crucially, since there are no free Fe^{3+} ions in Fe-P water it is not possible to fill the gaps between particles by the growth of the additional Fe_2O_3 (via Eqs. 3 and 4) resulting in a discontinuous film seen in Fig. 6.

$$Ca(HCO_3)_2(aq) \rightleftharpoons Ca^{2+}(aq) + 2(HCO_3)^-(aq) \quad (1)$$

$$Ca(HCO_3)_2(aq) \rightarrow CaCO_3(s) + H_2O(l) + CO_2(g) \quad (2)$$

$$Fe(OH)_3(aq) \rightleftharpoons Fe^{3+}(aq) + 3(OH)^-(aq) \quad (3)$$

$$2Fe(OH)_3(aq) \rightarrow Fe_2O_3(s) + 3H_2O(aq) \quad (4)$$

$$Cu(OH)_2(aq) \rightleftharpoons Cu^{2+}(aq) + 2(OH)^-(aq) \quad (5)$$

$$Cu(OH)_2(aq) \rightarrow CuO(s) + H_2O(aq) \quad (6)$$

3.5. Passivation phenomena in real-world used kettles

To demonstrate the natural occurrence of these passivation films, used kettles were randomly collected from soft water (Dublin, hardness around 50 mg/L as $CaCO_3$) and hard water (Kildare, around 170 mg/L as $CaCO_3$) supply regions, respectively (information listed in Table 2). Raman spectroscopic analysis confirms that calcium (II) carbonate ($CaCO_3$) and copper (II) oxide (CuO) films formed on the surfaces of the used kettles from hard water and soft water supply regions, respectively

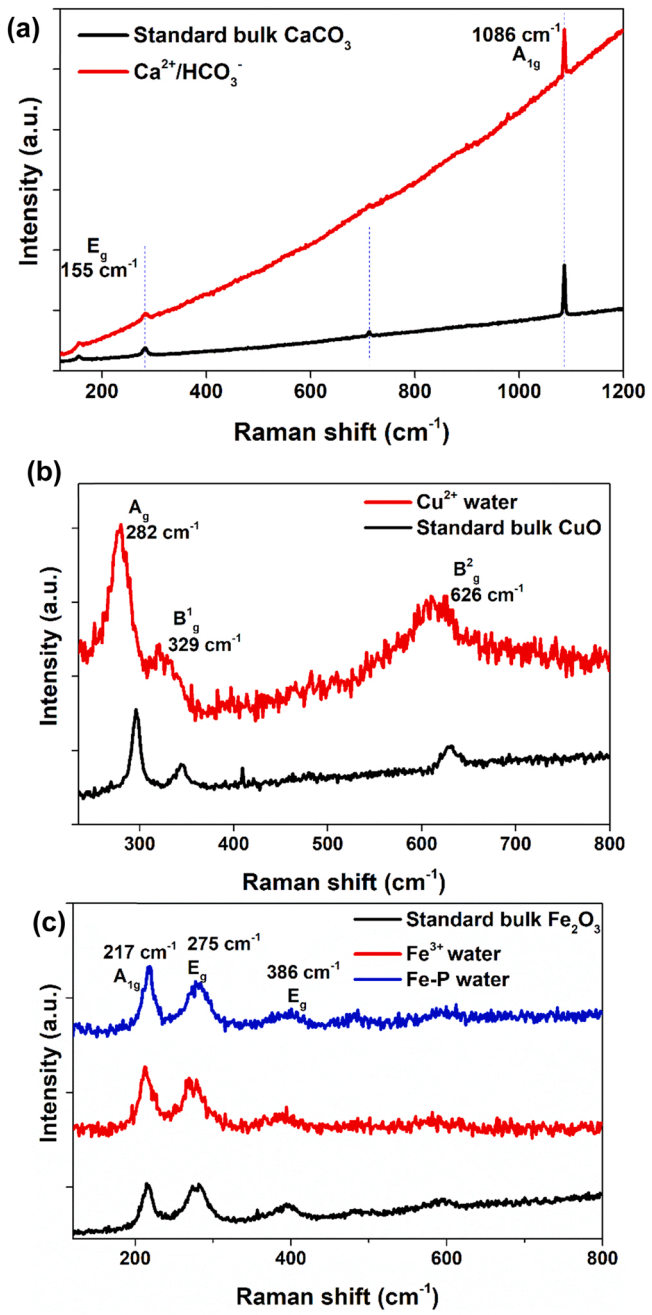

Fig. 9. (a) Raman spectra of standard CaCO3 powder and the particles from Ca^{2+}/HCO_3^- water boiled kettle, respectively. (b) Raman spectra of standard CuO powder and the particles from Cu^{2+} water boiled kettle, respectively. (c) Raman spectra of standard Fe_2O_3 powder and the particles from Fe^{3+} water and Fe-P water boiled kettle, respectively.

(Fig. 10a and b).

To assess the MP controlling effect, brand new kettles of the same type were purchased and tested. MP release levels from the brand new and used kettles were measured following the protocol in Fig. 2b. In contrast to MP release levels from brand-new kettles, the MP release from used kettles collected from hard water and soft water region were reduced by 56.6% and 88.7%, respectively (Fig. 10c). These results are consistent with the results obtained using SDW, which confirms that naturally formed passivation films can effectively reduce MP release.

4. Discussion

This study underscores the substantial influence of water constituents, e.g., ions and particles species on MP release levels during practical use. Based on this study, the MP release mitigation efficiency ranking is $Fe^{3+} \approx Cu^{2+} > Ca^{2+}/HCO_3^- > > Fe_2O_3$ particle ≈ DI water (Figs. 3 and 4). Because Fe^{3+} and Cu^{2+} ions in water can react to form the corresponding insoluble metal oxides, a passivation film forms that covers the surface of plastic and reduces MP release levels by 96.9% and 94.5% respectively. For hardwater, dense calcium carbonate crystals covered large area of the kettle surface. These rod-like crystals were quite large, with length around 10–100 μm, which is consistent with a previous publication (Roque et al., 2004). As a result, the inevitable presence of gaps between these crystals may reduce the suppression efficiency, though it can still reduce MP release by 89.7%. Particles of Fe_2O_3 (97% particles ranging 1.2–16 μm, and very similar to the particles size distribution found in drinking water (Pronk et al., 2007)) achieved the lowest control efficiency due to the lack of a continuous passivation film. Interestingly, we find an approximate 50% reduction in MP release when initially exposing kettles to DI water, regardless of kettle brands and models. This indicates that the typical kettle manufacturing process may result in formation of a large number of loosely bound surface particles, which boost the initial MP release levels. However, further studies are required to fully understand the original of the initial reduction observed in the case of DI water exposed kettles.

Based on these results it is expected that the levels of MP release from daily-use plastic products that come into contact with water will vary from region to region due to the different constituents in local drinking water. For example, in regions with hard water (Kildare), the presence of $CaCO_3$ films on the interior of used kettles is not unexpected (MacAdam and Parsons, 2004). In the case of the soft water zones (Dublin), we observed the formation of CuO-based films inside of used kettles (Fig. 10). Tests of Dublin tap drinking water found the concentration of copper to be around 0.5–0.8 mg/L, which is likely due to the widespread use of copper plumbing. The different types of films formed inside of real used kettles is therefore consistent with our study using synthetic waters. At worldwide level, there are even larger variations in the types and concentrations of constituents found in local drinking water. A comprehensive study (Hori et al., 2021) found that the mean hardness of tap drinking water varies from 49 ± 26 mg/L-$CaCO_3$ in Japan, to around 187 ± 71 mg/L in Germany and 362 ± 112 mg/L in Zambia. In addition to soft/hard water sources, local preferences for plumbing material can also significantly influence metal concentration in drinking water. Copper plumbing is widely used in developed countries, which leads to the high concentration of Cu ions in drinking water. It was reported that average copper concentration in British Columbia (Canada, school taps) was around 3.6 mg/L (Barn et al., 2014) while in California this value was around 0.2 mg/L (Kimbrough, 2007). In contrast, this value in Shanghai (China) was only around 0.01 mg/L (Xu et al., 2006). Evidently, differences in these water constituents will influence the film type, thickness and morphology formed on plastic surfaces, which will ultimately lead to variations in MP release levels. Ultimately, generated MPs are either discharged into waterways or consumed by local people, which leads to different human health and environmental risks. Given the impact of water constituents on MP release (Figs. 3 and 4), to achieve reliable estimates of the local levels of MP release it is vital to prepare the synthetic water that accurately mimics the local drinking water composition.

The natural passivation phenomenon reported here can substantially benefit the development of engineering solutions to control MP release. During the repeated boils using DI water, it was found that there was no leaching of Fe or Cu elements from Fe^{3+} and Cu^{2+} films, respectively (Table S1), while only tiny amount of $CaCO_3$ leached out. These results confirm that these naturally occurring oxide and carbonate-based films can withstand the typical adverse conditions experiences during daily use. It is interesting that we find that similar reduction efficiencies are

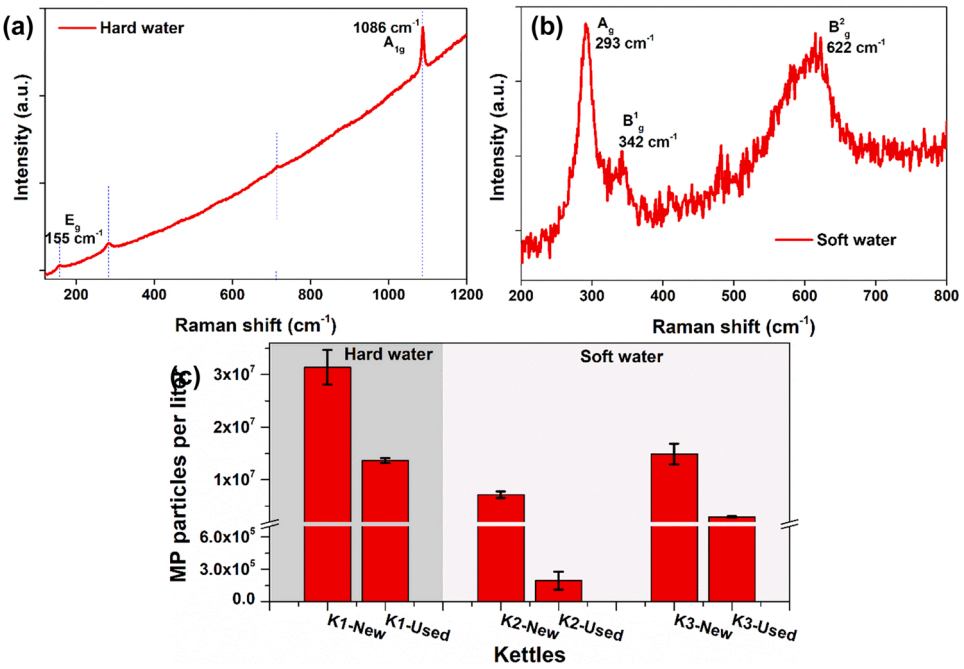

Fig. 10. (a) Raman spectra the surface particles of the used kettle collected from hard water zone-K1 in Table 2. (b) Raman spectra of the surface particles of the used kettle collected from soft water zone-K3 in Table 2. (C) MPs release number from brand-new and used kettles, respectively.

obtained from 2 transition metals: Fe^{3+} and Cu^{2+} (Fig. 3). This is due to their active transformation from metal ions into an insoluble metal oxide and suggests that other transition metals (ions speciation), such as Mn and Ti, may exhibit similar mitigation performance given the similar chemical transformation processes and the insoluble/slightly soluble nature of their metal oxides (Kozawa et al., 2011; Petlicki et al., 2005). In addition to the metal oxide, many other metallic carbonates (such as $FeCO_3$) are insoluble/slightly soluble in water and may also have potential to reduce MPs. Given the substantial influence of chemical speciation (particle/ion) on film formation and MP release suppression (Figs. 3–6), any engineered coating solution should start from ions in solution rather than particles, due to the benefits of forming a continuous passivating film. In addition, other coating parameters and conditions, such as water pH, ion solute concentration, reaction pressure and potential catalysts may also influence the reaction efficiency, and control crystal size, which subsequently determines the film thickness and robustness. Hence, these parameters and conditions need to be optimized to generate the highest-performance films. Overall, this nature inspired engineering solutions demonstrate great potential to mitigate against MP release from daily-use plastics.

5. Conclusions

In the present study, the influence of typical drinking water ions (Ca^{2+}/HCO_3^-; Fe^{3+} and Cu^{2+}) and particles (Fe_2O_3 particles) on MP release was systematically investigated. Surprisingly, all ions resulted in a greater than 89% reduction in MP release while particles showed no significant effect compared to the DI water control. We find that the MP release suppression efficiency ranking is $Fe^{3+} \approx Cu^{2+} > Ca^{2+}/HCO_3^- >> Fe_2O_3$ particles $\approx$ DI water. Physical and chemical characterization using SEM-EDX, AFM, XPS and Raman spectroscopy confirmed the ions in hard water (Ca^{2+}/HCO_3), and water containing Cu^{2+} and Fe^{3+} ions respectively resulted in the formation of $CaCO_3$, CuO, and Fe_2O_3 passivation films on the exposed kettle surface, each of which led to a substantial reduction in MP release level over that found for DI water. In contrast, no film was formed when the plastic was exposed to the synthetic water with particles (Fe_2O_3) in water. Additionally, we showed that films with different chemical compositions can form naturally in the kettles used in real life due to different ions present in regional water supplies. This study underscores the substantial influence of water constituents on regional MP release and human exposure. More importantly, the natural passivation phenomenon reported here can hugely benefit the development of engineering methods to control MP release.

CRediT authorship contribution statement

Jing Jing Wang: Conceptualization, Review & editing, Supervision. **Liwen Xiao**: Conceptualization, Review & editing, Supervision. **John J. Boland**: Conceptualization, Review & editing, Supervision. **Yunhong Shi**: Investigation, Methodology, Data collection & analysis, Writing–original draft. **Dunzhu Li**: Investigation, Validation, Analysis, Writing – original draft. **Emmet D. Sheerin**: Investigation and Analysis (SEM-EDX), Proofreading. **Daragh Mullarkey**: Investigation and analysis (XPS). **Luming Yang**: Investigation. **Xue Bai**: Investigation. **Igor V. Shvets**: Investigation (XPS).

Declaration of Competing Interest

The authors declare that they have no known competing financial interests or personal relationships that could have appeared to influence the work reported in this paper.

Acknowledgments

We appreciate the professional helps from Prof. Sarah Mc Cormack and technician teams (David A. McAulay, Mary O'Shea, Patrick L.K. Veale and Mark Gilligan etc.) of Trinity Civil, Structural and Environmental Department and Photonics Laboratory and AML in CRANN/AMBER Research Centre. The presentation of the material in this publication does not imply the expression of any opinion whatsoever on the part of Trinity College Dublin about specific companies or of certain manufacturers' products and does not imply that they are endorsed, recommended, criticised or otherwise by Trinity College Dublin in preference to others of a similar nature. Errors and omissions excepted. All reasonable precautions have been taken to verify the information contained in this publication. However, the published material is being

This work was supported by Enterprise Ireland (grant number CF20180870), Ireland; Science Foundation Ireland (grants numbers: 20/FIP/PL/8733, 12/RC/2278_P2 and 16/IA/4462), Ireland; the School of Engineering Scholarship at Trinity College Dublin, and the China Scholarship Council (201506210089 and 201608300005), China. D.M. and I.V.S acknowledge support of Irish Research Council Laureate Award (IRCLA/2019/171). Ireland.

Appendix A. Supporting information

Supplementary data associated with this article can be found in the online version at doi:10.1016/j.jhazmat.2021.127997.

References

Barn, P., Nicol, A.-M., Struck, S., Dosanjh, S., Li, R., Kosatsky, T., 2014. Investigating elevated copper and lead levels in school drinking water. Environ. Health Rev. 56 (04), 96–102.

Biesinger, M.C., Lau, L.W., Gerson, A.R., Smart, R.S.C., 2010. Resolving surface chemical states in XPS analysis of first row transition metals, oxides and hydroxides: Sc, Ti, V, Cu and Zn. Appl. Surf. Sci. 257 (3), 887–898.

Biesinger, M.C., Payne, B.P., Grosvenor, A.P., Lau, L.W., Gerson, A.R., Smart, R.S.C., 2011. Resolving surface chemical states in XPS analysis of first row transition metals, oxides and hydroxides: Cr, Mn, Fe, Co and Ni. Appl. Surf. Sci. 257 (7), 2717–2730.

Briggs, J.C. and Ficke, J.F., 1977. Quality of rivers of the United States, 1975 water year: Based on the National Stream Quality Accounting Network (NASQAN), US Geological Survey.

Du, F., Cai, H., Zhang, Q., Chen, Q., Shi, H., 2020. Microplastics in take-out food containers. J. Hazard Mater. 399, 122969.

Fadare, O.O., Wan, B., Guo, L.-H., Zhao, L., 2020. Microplastics from consumer plastic food containers: Are we consuming it? Chemosphere 253, 126787.

Galloway, T.S., Cole, M., Lewis, C., 2017. Interactions of microplastic debris throughout the marine ecosystem. Nat. Ecol. Evol. 1 (5), 1–8.

He, Y.-J., Qin, Y., Zhang, T.-L., Zhu, Y.-Y., Wang, Z.-J., Zhou, Z.-S., Xie, T.-Z., Luo, X.-D., 2021. Migration of (non-) intentionally added substances and microplastics from microwavable plastic food containers. J. Hazard Mater. 417, 126074.

Hernandez, L.M., Xu, E.G., Larsson, H.C., Tahara, R., Maisuria, V.B., Tufenkji, N., 2019. Plastic teabags release billions of microparticles and nanoparticles into tea. Environ. Sci. Technol. 53 (21), 12300–12310.

Hori, M., Shozugawa, K., Sugimori, K., Watanabe, Y., 2021. A survey of monitoring tap water hardness in Japan and its distribution patterns. Sci. Rep. 11 (1), 1–13.

Ibrahim, Y.S., Tuan Anuar, S., Azmi, A.A., Wan Mohd Khalik, W.M.A., Lehata, S., Hamzah, S.R., Ismail, D., Ma, Z.F., Dzulkarnaen, A., Zakaria, Z., 2021. Detection of microplastics in human colectomy specimens. JGH Open 5 (1), 116–121.

Jin, Y., Lu, L., Tu, W., Luo, T., Fu, Z., 2019. Impacts of polystyrene microplastic on the gut barrier, microbiota and metabolism of mice. Sci. Total Environ. 649, 308–317.

Käppler, A., Fischer, D., Oberbeckmann, S., Schernewski, G., Labrenz, M., Eichhorn, K.-J., Voit, B., 2016. Analysis of environmental microplastics by vibrational microspectroscopy: FTIR, Raman or both? Anal. Bioanal. Chem. 408 (29), 8377–8391.

Kimbrough, D.E., 2007. Brass corrosion as a source of lead and copper in traditional and all-plastic distribution systems. J. Water Works Assoc. 99 (8), 70–76.

Kozawa, T., Onda, A., Yanagisawa, K., Kishi, A., Masuda, Y., 2011. Effect of water vapor on the thermal decomposition process of zinc hydroxide chloride and crystal growth of zinc oxide. J. Solid State Chem. 184 (3), 589–596.

Li, D., Shi, Y., Yang, L., Xiao, L., Kehoe, D.K., Gun'ko, Y.K., Boland, J.J., Wang, J.J., 2020. Microplastic release from the degradation of polypropylene feeding bottles during infant formula preparation. Nat. Food 1, 746–754.

Li, D., Yang, L., Kavanagh, R., Xiao, L., Shi, Y., Kehoe, D.K., Sheerin, E.D., Gun'ko, Y.K., Boland, J.J., Wang, J.J., 2021. Sampling, identification and characterization of microplastics release from polypropylene baby feeding bottle during daily use. JoVE 18, e62545.

Lu, L., Wan, Z., Luo, T., Fu, Z., Jin, Y., 2018. Polystyrene microplastics induce gut microbiota dysbiosis and hepatic lipid metabolism disorder in mice. Sci. Total Environ. 631, 449–458.

MacAdam, J., Parsons, S.A., 2004. Calcium carbonate scale formation and control. Rev. Environ. Sci. Bio/Technol. 3 (2), 159–169.

Mattsson, K., Johnson, E.V., Malmendal, A., Linse, S., Hansson, L.-A., Cedervall, T., 2017. Brain damage and behavioural disorders in fish induced by plastic nanoparticles delivered through the food chain. Sci. Rep. 7 (1), 11452.

Murray, D., Liao, J., Stankovic, L., Stankovic, V., 2016. Understanding usage patterns of electric kettle and energy saving potential. Appl. Energy 171, 231–242.

Murthy, P.S., Venugopalan, V., Arunya, D.D., Dhara, S., Pandiyan, R. and Tyagi, A., 2011, Antibiofilm activity of nano sized CuO, pp. 580–583, IEEE.

Petlicki, J., Palusova, D., van de Ven, T.G., 2005. Physicochemical aspects of catalytic decomposition of hydrogen peroxide by manganese compounds. Ind. Eng. Chem. Res. 44 (7), 2002–2010.

Pronk, M., Goldscheider, N., Zopfi, J., 2007. Particle-size distribution as indicator for fecal bacteria contamination of drinking water from karst springs. Environ. Sci. Technol. 41 (24), 8400–8405.

Ragusa, A., Svelato, A., Santacroce, C., Catalano, P., Notarstefano, V., Carnevali, O., Papa, F., Rongioletti, M.C.A., Baiocco, F., Draghi, S., 2021. Plasticenta: first evidence of microplastics in human placenta. Environ. Int. 146, 106274.

Ramsperger, A., Narayana, V., Gross, W., Mohanraj, J., Thelakkat, M., Greiner, A., Schmalz, H., Kress, H., Laforsch, C., 2020. Environmental exposure enhances the internalization of microplastic particles into cells. Sci. Adv. 6 (50), eabd1211.

Ranjan, V.P., Joseph, A., Goel, S., 2020. Microplastics and other harmful substances released from disposable paper cups into hot water. J. Hazard Mater. 404, 124118.

Roque, J., Molera, J., Vendrell-Saz, M., Salvadó, N., 2004. Crystal size distributions of induced calcium carbonate crystals in polyaspartic acid and Mytilus edulis acidic organic proteins aqueous solutions. J. Cryst. Growth 262 (1–4), 543–553.

Sarin, P., Snoeyink, V., Lytle, D., Kriven, W., 2004. Iron corrosion scales: model for scale growth, iron release, and colored water formation. J. Environ. Eng. 130 (4), 364–373.

Schwabl, P., Köppel, S., Königshofer, P., Bucsics, T., Trauner, M., Reiberger, T., Liebmann, B., 2019. Detection of various microplastics in human stool: a prospective case Series. Ann. Intern. Med. 171 (7), 453–457.

Shackery, I., Patil, U., Pezeshki, A., Shinde, N.M., Kang, S., Im, S., Jun, S.C., 2016. Copper hydroxide nanorods decorated porous graphene foam electrodes for non-enzymatic glucose sensing. Electrochim. Acta 191, 954–961.

Sturm, M.T., Kluczka, S., Wilde, A. and Schuhen, K., 2019. Determination of particles produced during boiling in differenz plastic and glass kettles via comparative dynamic image analysis using FlowCam®.

Van der Laan, G., Westra, C., Haas, C., Sawatzky, G., 1981. Satellite structure in photoelectron and Auger spectra of copper dihalides. Phys. Rev. B 23 (9), 4369–4380.

Wang, L., Gupta, K., Goodall, J.B., Darr, J.A., Holt, K.B., 2017. In situ spectroscopic monitoring of CO_2 reduction at copper oxide electrode. Faraday Discuss. 197, 517–532.

WHO, 2006, Standards for materials used in plumbing systems, Geneva, Switzerland.

WHO, 2011, Guidelines for drinking-water quality, 4th edition.

Xu, J., Ji, W., Shen, Z., Li, W., Tang, S., Ye, X., Jia, D., Xin, X., 1999. Raman spectra of CuO nanocrystals. J. Raman Spectrosc. 30 (5), 413–415.

Xu, P., Huang, S., Wang, Z., Lagos, G., 2006. Daily intakes of copper, zinc and arsenic in drinking water by population of Shanghai, China. Sci. Total Environ. 362 (1–3), 50–55.

Yu, T., Zhao, X., Shen, Z., Wu, Y., Su, W., 2004. Investigation of individual CuO nanorods by polarized micro-Raman scattering. J. Cryst. Growth 268 (3–4), 590–595.